Functional degeneracy in translationally active *Nitrospira* populations confers resilience to out-selection in partial nitritation activated sludge

Maxwell B.W. Madill[1,+], Yaqian Luo[1,+], Pranav Sampara[1], Ryan M. Ziels[1*]

[1] Department of Civil Engineering, University of British Columbia, Vancouver, Canada

[+] Contributed equally to this work.

* Corresponding Author:
Email: ziels@mail.ubc.ca

Abstract

Energy-efficient nitrogen removal in activated sludge wastewater treatment systems could be achieved by oxidizing a part of the influent ammonium to nitrite (partial nitritation; PN) to provide growth substrates for anammox. However, the metabolic and physiological diversity of nitrite oxidizing bacteria (NOB) makes their out-selection a challenge in mainstream activated sludge, warranting measurements of their *in situ* physiology and activity under selective growth pressures. Here, we examined the long-term (~100 day) stability of PN in mainstream activated sludge obtained by treating a portion of return activated sludge with a sidestream flow containing free ammonia (FA) at 200 mg NH_3-N/L. The nitrite accumulation ratio peaked at 42% by day 40 in the reactor with sidestream FA-treatment, while it did not increase in the control reactor without FA added to the sidestream. A subsequent decrease in nitrite accumulation within the FA-treated reactor coincided with shifts in dominant *Nitrospira* 16S rRNA amplicon sequence variants (ASVs). We applied bioorthogonal non-canonical amino acid tagging (BONCAT) coupled with fluorescence activated cell sorting (FACS) to investigate changes in the translational activity of NOB populations throughout sidestream exposure to FA. BONCAT-FACS confirmed that the single *Nitrospira* ASV out-selected in the FA-treated reactor had reduced translational activity following exposure to FA, whereas the two *Nitrospira* ASVs that emerged after process acclimation were not impacted by FA. Thus, functionally degenerate *Nitrospira* populations likely provided resilience to the nitrite-oxidizing community during FA-treatment by shifting activity to physiologically resistant members. These results highlight how *in situ* physiology approaches like BONCAT can resolve ecological niches in the activated sludge microbiome, and how functional degeneracy observed within *Nitrospira* populations likely necessitates a combination of out-selection strategies to achieve stable mainstream PN.

Keywords: partial nitritation, nitrification, activated sludge, microbiome, BONCAT, nitrite oxidation

1. Introduction

Net-energy neutral or positive wastewater treatment can be achieved by decoupling carbon and nitrogen removal in A-B type treatment schemes designed to maximize energy recovery by shunting COD towards anaerobic processes while utilizing carbon and energy efficient biological nitrogen removal (BNR) processes (Cogert et al., 2019). Pairing partial nitritation (PN) with anaerobic ammonium oxidation (anammox) yields a completely autotrophic BNR process (PN–anammox, or PN-A) that offers significant reductions in COD and aeration requirements compared to conventional BNR (Li et al., 2018). While PN-A shows promise as a B-Stage BNR process to follow upstream carbon-capturing A-stage processes, achieving stable PN in mainstream activated sludge (AS) stands as a major challenge limiting its successful full-scale implementation (Regmi et al., 2014; Xu et al., 2015).

Achieving stable PN relies on operating strategies that consistently repress and wash-out (i.e. out-select) nitrite oxidizing bacteria (NOB) while maintaining ammonium oxidizing bacteria (AOB) within the system (Agrawal et al., 2018; Li et al., 2018). Preliminary success in mainstream NOB out-selection has been achieved using kinetic strategies that control nitrogen (Regmi et al., 2014) and oxygen (Ge et al., 2014; Kornaros et al., 2010; Regmi et al., 2014) substrate levels and/or availabilities to favour the growth kinetics of AOB over NOB. Additionally, several recently-proposed side-stream return activated sludge (RAS) treatment strategies have achieved high efficiencies in selectively inhibiting NOB based on their higher innate sensitivity to free-ammonia (FA) and free-nitrous acid (FNA) compared to AOB (Cao et al., 2017; Duan et al., 2018; Wang et al., 2017). Wang et al. (2017) showed that RAS treatment with FA-rich sidestream wastewater typical of anaerobic digester centrate (210 mg NH_3-N/L) supported successful NOB out-selection in mainstream AS, with nitrite accumulation ratios reaching 80-90%. Despite its potential efficacy for supporting mainstream PN, a limited number of studies have further validated the long-term

68 stability of FA-based RAS treatment and assessed its impacts on the structure and activity of the
69 nitrifying microbial community (Duan et al., 2019a; Li et al., 2020).
70
71 NOB communities in wastewater treatment often display functional degeneracy, wherein the
72 nitrite oxidation process is distributed among several phylogenetically diverse taxa with varying
73 auxiliary metabolic potentials (Daims et al., 2016; Lücker et al., 2015; Spasov et al., 2019). Such
74 degeneracy may enable NOB communities to resist selective pressures imparted by out-selection
75 strategies by recruiting functionally redundant, yet physiologically diverse, NOB members (Duan
76 et al., 2019a; Li et al., 2020; Liu and Wang, 2013). *In situ* assessments of the metabolically active
77 fraction of nitrifying communities are therefore critical to elucidate the efficacy of mainstream NOB
78 out-selection strategies. Characterizing the microbial community using 16S ribosomal RNA
79 (rRNA) gene amplicon sequencing or shotgun metagenomics can illuminate how specific NOB
80 out-selection strategies alter community structure and functional potential (Nierychlo et al., 2020;
81 Singer et al., 2017). However, the genomic signature of a microbial community alone is not
82 necessarily predictive of the underlying *in situ* physiologies of active community members
83 (Hatzenpichler et al., 2020; Singer et al., 2017). While bulk activity measurements obtained
84 through metatranscriptomics, metaproteomics, or stable isotope probing can provide compelling
85 insights into the composition and function of the aggregate active microbial community, these
86 methods are currently unable to resolve the heterogeneity of community members often observed
87 at the cellular and/or strain level (Hatzenpichler et al., 2020, 2014).
88
89 Next-generation substrate analogue probing approaches have recently emerged as powerful
90 tools to decipher the *in situ* physiology of active cells based on their uptake of synthetic analogues
91 of natural biomolecules (Hatzenpichler et al., 2020). Bioorthogonal non-canonical amino acid
92 tagging (BONCAT) is a nascent SAP approach to study the physiology of active cells in complex
93 environmental microbiomes (Couradeau et al., 2019; Hatzenpichler et al., 2016, 2014; Reichart

94 et al., 2020). BONCAT relies on the *in vivo* uptake and incorporation of synthetic amino acids,
95 such as the alkyne-containing analogue of methionine, homopropargylglycine (HPG), into newly
96 synthesized proteins via the native translational machinery, and thereby selectively labels the
97 proteomes of translationally active cells (Hatzenpichler et al., 2014). HPG-labeled cells can
98 subsequently be identified by tagging their proteins with azide-modified fluorescent dyes via
99 azide-alkyne click-chemistry, enabling their selective recovery using fluorescence activated cell
100 sorting (FACS) (Couradeau et al., 2019; Hatzenpichler et al., 2016). To our knowledge, BONCAT,
101 or its paired approach with FACS (BONCAT-FACS), have yet to be applied to study the active
102 fractions of microbiomes central to wastewater treatment bioprocesses.
103
104 The objective of this study was to assess the stability of RAS treatment with FA as an NOB out-
105 selection strategy for mainstream PN. We hypothesized that certain members of the active
106 nitrifying microbial community could acclimate to routine FA exposure. We applied time-series
107 16S rRNA gene amplicon sequencing in addition to BONCAT-FACS based activity measurements
108 to elucidate the impact of FA-based RAS treatment on the structure and *in situ* activity of the AS
109 microbiome in parallel experimental and control sequencing batch reactors.
110
111
112 **2. Materials and Methods**
113
114 *2.1 Reactor setup, operation and monitoring*
115 Two identical lab-scale sequencing batch reactors (SBRs) with working volumes of 4.28 L were
116 seeded with AS from a pilot-scale SBR at a WWTP in King County (Washington, USA) (Figure
117 S1). The SBR cycles lasted 3 h, including 2 min aerobic feeding, 148 min aerobic reaction, 20
118 min settling, 5 min decanting, and 5 min idle periods. The SBR cycle timing was controlled with
119 ChronTrol XT timers (ChronTrol Corporation, California), and mixing was provided by overhead
120 mixers. Reactor temperature was maintained at 20 ± 1 ^{o}C using an environmental chamber. The

121 target solid retention times (SRTs) were kept at 10 days for both SBRs throughout the study by
122 wasting a determined amount of biomass based on daily measurements of mixed liquor and
123 effluent total suspended solids (TSS) and volatile suspended solids (VSS). The SBRs were fed
124 with a synthetic wastewater containing ammonium chloride as the nitrogen source and sodium
125 acetate and propionic acid as organic carbon sources, producing 24.5 ± 2 mg NH_4-N/L and 100
126 ± 37 mg/L of soluble chemical oxygen demand (sCOD), respectively. Macro and micro element
127 components of the synthetic wastewater are detailed in the Supplementary Information.

128 Two operational phases were sequentially conducted: the Start-up Phase and the FA Phase. In
129 the Start-up Phase, the two SBRs were operated under the same aerobic conditions without FA-
130 treatment of RAS to achieve similar nitrification performance. The SBRs were fed with 1.07 L of
131 synthetic wastewater in each SBR cycle using peristaltic pumps (LabF1/YZ1515, Shenchen
132 Precision Pump, China), resulting in a hydraulic retention time (HRT) of 12 h. The pH was not
133 controlled but measured within the range of 6.7-7.5. Aeration was provided by an air pump and
134 dissolved oxygen ranged from 3-8 mg/L in a typical SBR cycle. The Start-up Phase lasted 274
135 days to establish steady-state conditions.

136 The FA Phase was commenced on day 275, hereafter referred to as 'day zero', and lasted 94
137 days. The operational conditions in the FA Phase were similar to those in the Start-up Phase,
138 except for the following differences (Figure S1). In the FA Phase, 800 mL of mixed liquor was
139 removed from each SBR at the end of the reaction period of a given cycle every 24 h, and was
140 thickened to 50 mL by centrifugation. The thickened RAS was incubated in an unstirred 200 mL
141 beaker containing 100 mL of media with the same composition as the synthetic feed, but with no
142 COD. For the experimental reactor, hereafter termed the FA-treated SBR, the RAS treatment
143 solution contained 1060 mg/L NH_4-N, with pH adjusted to 9 using sodium hydroxide to produce a
144 final FA concentration of 200 mg NH_3-N/L characteristic of anaerobic digester centrate. In the
145 other reactor, hereafter termed the control SBR, thickened RAS was incubated in the same

146 medium at a pH of 9 but without ammonium addition. After 24 h of incubation, the 150 mL of
147 treated RAS was recycled back into the respective SBRs at the start of the next cycle. To maintain
148 consistent nitrogen loadings in the two SBRs, 0.406 g of ammonium chloride was added to the
149 control SBR simultaneously with the treated RAS. Monitoring experiments lasting 24 h were
150 performed approximately every 10 days to measure composite daily nitrite accumulation ratios
151 (NARs), as described in the Supplementary Information.

152 During the FA Phase, effluent nutrient samples were collected just before the addition of treated
153 RAS. Nitrogen species (ammonium, nitrite, and nitrate), orthophosphate, and soluble COD
154 (sCOD) in effluent samples were monitored three to four times per week. pH and DO were
155 measured at least three times per week. Analytical methods for bioreactor monitoring are
156 described in Table S1.

157 *2.2 Microcosms for bioorthogonal non-canonical amino acid tagging (BONCAT)*

158 Three 30 mL samples were collected from each SBR throughout the RAS treatment cycle
159 commenced on day 94, including: (1) a mixed liquor sample immediately preceding bulk mixed
160 liquor removal for RAS treatment; (2) a RAS sample after 15 min of side-stream treatment (S1);
161 and (3) a RAS sample after 24 h of side-stream treatment (S2). The treated RAS samples were
162 volume-corrected for the thickening process to attain the same biomass concentrations as the
163 mixed liquor samples. Samples were washed in phosphate buffered saline (1x PBS; filter
164 sterilized) through centrifugation (3000 rpm, 5 min) and resuspension to remove residual growth
165 substrates. All samples were incubated in a media consisting of 25% synthetic wastewater in 1x
166 PBS (vol/vol) without COD or yeast extract, so that NH_4-N was the only exogenous electron donor.
167 For BONCAT-labeling microcosms, 15 mL portions of each sample were resuspended in 15 mL
168 of incubation media amended with 1 mM homopropargylglycine (HPG; Click Chemistry Tools,

169 Arizona) (HPG-positive microcosm), transferred into sterile 125 mL Erlenmeyer flasks, and
170 incubated on an orbital shaker for 3 h at 20 °C and 200 rpm. Control microcosms (HPG-negative)
171 for each sample were conducted similarly except without HPG amendment. Following
172 incubations, microcosm samples were washed three times in 1x PBS to remove unincorporated
173 HPG, resuspended in 10% (vol/vol) glycerol in PBS, aliquoted into 1 mL and stored at -80°C until
174 further processing. Details on how the preliminary BONCAT validation microcosms were
175 conducted are provided in the Supplementary Information.

176 *2.3 BONCAT Sample Preparation and Click-Chemistry*

177 For each microcosm type (R, S1, or S2) for both SBRs, sample preparation and click-chemistry
178 were conducted using triplicate HPG-positive and duplicate HPG-negative microcosm samples.
179 Samples were thawed on ice at 4 °C, enzymatically homogenized, subjected to filter-immobilized
180 click-chemistry labeling with the FAM picolyl azide dye (Click Chemistry Tools) closely following
181 the procedure of Couradeau et al. (2019), detached from the filter, pre-strained through a 30 um
182 mesh filter, and counterstained with SYTO59 (10,000x final dilution; ThermoFisher Scientific,
183 Oregon) to generate the pre-sort samples for FACS. Details of the sample homogenization and
184 click-chemistry labeling procedures are provided in the Supplementary Information.

185 *2.4 Fluorescence-activated cell sorting (FACS)*
186
187 Fluorescence-activated cell sorting was conducted on a BD FACSJazz™ cell sorter (BD
188 Biosciences, California) calibrated to detect the FAM picolyl azide dye (excitation = 490
189 nm/emission = 510 nm) and the SYTO59 counterstain dye (excitation = 622 nm/emission = 645
190 nm). An overview of the FACS gating procedures is provided in the Supplementary Information.
191 Briefly, initial gating was established with side-scatter, forward-scatter and trigger pulse width to

192 exclude large particles and cell aggregates. Sorting gates were set targeting BONCAT-positive
193 (BONCAT+) cell fractions based on background SYTO59 and FAM fluorescence, allowing less
194 than 0.5% of false positives (Figures S2-S6). A total of 100k cells were analyzed from each
195 sample, where cells within the sorting gate (SYTO+, BONCAT+) were sorted into 1.5 mL tubes
196 containing 400 µL of prepGEM Wash Buffer (ZyGEM™, Virginia), and stored at -80 °C until further
197 analysis.

198
199
200 *2.5 DNA Extraction and 16S rRNA gene amplicon sequencing*
201
202 For time-series analysis of community composition, triplicate 980 µL aliquots of mixed liquor were
203 routinely collected directly from the SBRs at the end of a cycle and flash frozen at -80 °C. Mixed
204 liquor samples were thawed on ice, and DNA was extracted using the FastDNA Spin Kit for Soil
205 (MP Biomedicals, Santa Ana) with minor modifications (Nierychlo et al., 2020). For each HPG-
206 positive microcosm type (R, S1, or S2) for both SBRs, 50 µL aliquots were collected from the
207 triplicate pre-homogenized and pre-sort samples during preparation for FACS, added to 400 µL
208 of prepGEM Wash Buffer, and stored at -80 °C. Pre-homogenized samples from HPG-negative
209 R microcosms and bulk mixed liquor samples were prepared similarly. All pre-homogenized, pre-
210 sort, and BONCAT-FACS samples were extracted using the prepGEM Bacteria kit (ZyGEM™)
211 using a low-biomass input procedure overviewed in the Supplementary Information. DNA
212 concentrations were measured with the Qubit® dsDNA BR and HS Assay Kits and Qubit®
213 fluorometer (ThermoFisher Scientific, Oregon).

214
215 16S rRNA gene fragments from all DNA extracts were amplified using barcoded primers, 515F
216 and 926R (Parada et al., 2016), targeting the V4-V5 hypervariable region of the 16S rRNA gene.
217 All samples extracted with the prepGEM kit underwent an initial round of 15-cycles of PCR with
218 non-barcoded 515F and 926R primers due to the low-biomass input. One triplicate set of FastDNA

extracts from day 94 were also pre-amplified to determine potential biases of that step. Amplified barcoded PCR products were pooled at equimolar concentrations and sequenced on an Illumina MiSeq in paired-end 300 bp mode at the UBC Biofactorial facility.

Amplicon reads were processed and denoised into amplicon sequencing variants (ASVs) with DADA2 (Callahan et al., 2016) (v.1.12.1) in the R environment. The script used to generate the ASV datasets is provided in Supplementary Information. Denoised sequences were taxonomically classified using the RDB Classifier (Wang et al., 2007) against the MiDAS 3.0 database (Nierychlo et al., 2020). The raw read files are available via the NCBI Short Read Archive under BioProject PRJNA693634.

2.5 Statistical analysis

Comparisons of reactor nutrient data were performed with t-tests for N-of-1 trials with serial correlation (Tang and Landes, 2020). Amplicon sequencing data was visualized using the tidyverse package (Wickham et al., 2019) (v.1.3.0) in the R environment. Principal component analysis (PCA) of log-transformed cumulative-sum scaled (CSS) ASV read counts was performed using the metagenomeSeq (Paulson et al., 2013) (v.1.26.3) and vegan (Oksanen et al., 2007) (v.2.5.6) packages in R. PERMANOVA (adonis) was conducted in vegan with 1000 permutations to determine significant differences in reactor communities over time. Differential abundance analysis of ASVs between SBRs and in BONCAT microcosm datasets was performed using DESeq2 (Love et al., 2014) (v.1.24.0) using parametric fitting, the Wald significance test, and Benjamin-Hochberg correction for *p* values. FACS data was processed using the flowcore package (v.1.52.1) (Hahne et al., 2009) in R.

247 **3. Results**
248
249 *3.1 Partial nitritation performance of activated sludge bioreactors*
250
251 The two SBRs treated simulated mainstream municipal wastewater over two operational phases:
252 the Start-up Phase and the FA Phase. Steady-state conditions were presumed over the last 30
253 days of the 270-day Start-up Phase, during which daily effluent concentrations of NH_4-N, NO_3-N,
254 and NO_2-N were similar in the two SBRs ($p > 0.05$), and averaged 0.1±0.3 mg NH_4-N/L, 19±2
255 mg NO_3-N/L and 0.0±0.01 mg NO_2-N/L, respectively (Figure 1). The TSS and VSS of mixed liquor
256 were also similar between the two systems during the Start-up Phase ($p > 0.05$; Figure S7). Thus,
257 similar stable performance with full nitrification was achieved in both SBRs during the initial Start-
258 up Phase, indicating effective duplication of operating conditions.
259
260 The FA Phase was then commenced on day 0 to assess the efficacy of FA-treatment of RAS for
261 promoting stable mainstream PN and observe its impacts on microbial community structure and
262 activity. After 10 days of sidestream RAS treatment, NO_2-N began to increase in effluent of the
263 FA-treated SBR, but stayed below detection in the control SBR for the remainder of the FA Phase
264 (Figure 1). By day 40, effluent NO_2-N reached its peak level of 11 mg NO_2-N/L in the FA-treated
265 SBR. At the same time, NH_4-N accumulated to 3.7 mg NH_4-N/L in the FA-treated SBR between
266 days 37 and 44, yet stayed below 1.2 mg NH_4-N/L in the control SBR over the entire FA Phase
267 (Figure 1). The accumulation of NO_2-N in the FA-treated SBR was transient, however, as the
268 effluent concentration decreased after day 40 and reached a value below detection by day 74
269 (Figure 1).
270
271 Because effluent was sampled from the SBRs on a 24 h basis, and the sidestream-treated RAS
272 was added once every 24 h, periodic tests were conducted to measure nitrogen species at the
273 end of individual SBR cycles over the course of 24 h to better estimate nitrite accumulation ratios

274 (NARs) (Figure S8). After 20 days of FA-treatment, the 24 h average NAR was approximately 10
275 times higher in the FA-treated SBR versus the control (Figure 1C). The NAR reached its peak of
276 41.9% by day 37 in the FA-treated SBR, aligning with the observed peak in effluent NO_2-N. The
277 NAR of the control SBR stayed below 3.2% in the entire FA Phase (Figure 1C). This suggests
278 that the efficacy of RAS treatment with FA as a strategy to promote PN in mainstream AS is
279 subject to microbial acclimation, as the extent of nitrite oxidation inhibition was not sustained after
280 40 days.

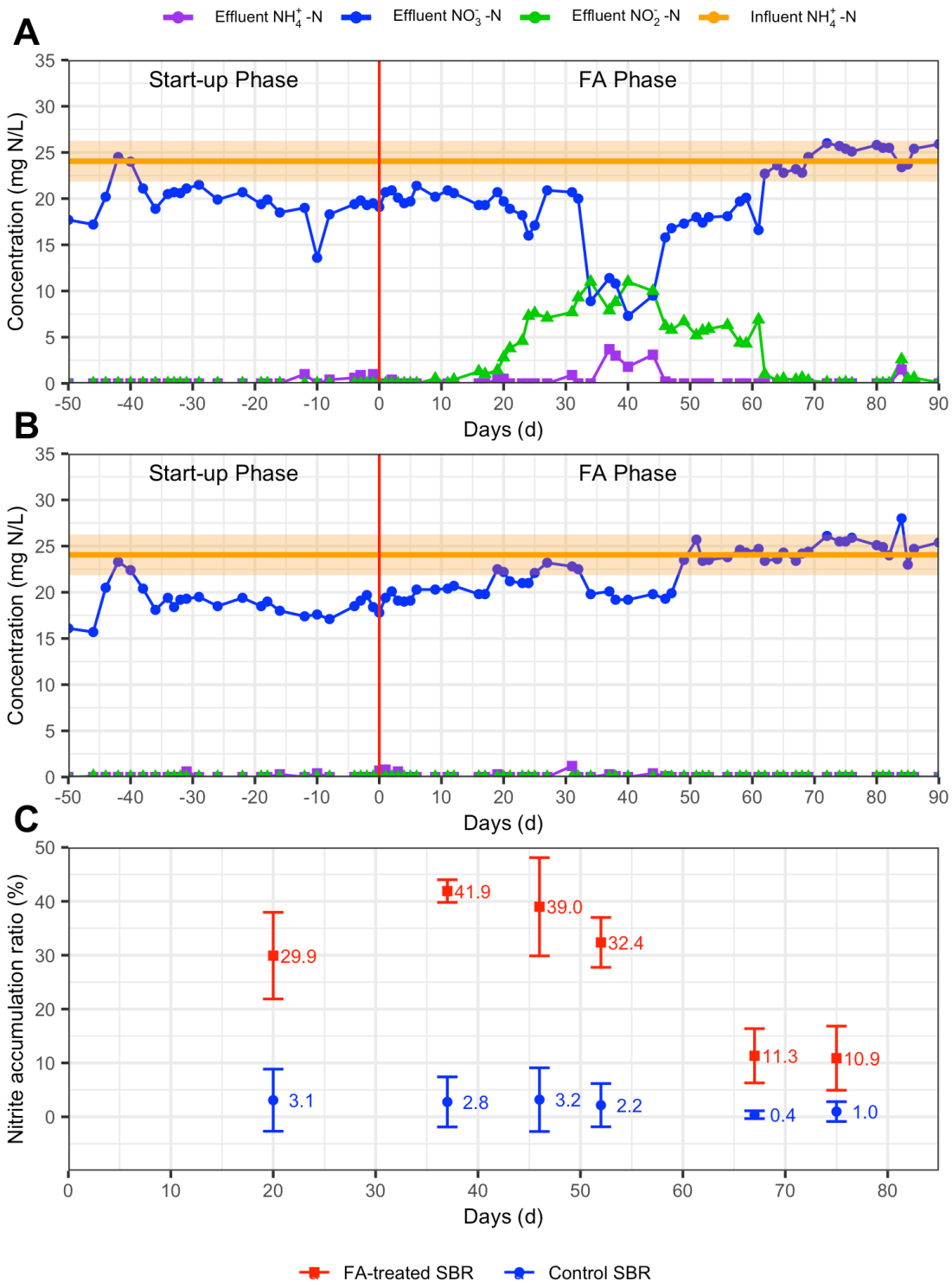

Figure 1: Influent and effluent nitrogen species over the two experimental phases in (A) free-ammonia (FA) treated sequencing batch reactor (SBR), and (B) control SBR. Shaded orange space represents standard deviation of influent NH_4-N. (C) Nitrite accumulation ratio (NAR, %) of FA-treated and control SBRs over time, based on 24 h monitoring of SBR effluents.

3.2 Microbial community acclimation to FA-treatment

Microbial 16S rRNA gene amplicons were denoised into ASVs to provide a high-resolution (Callahan et al., 2016; Eren et al., 2015) view of how RAS treatment impacted community structure. A total of 3.01 million chimera-free quality-filtered merged reads (Table S2) were denoised into 6,694 ASVs. Over 95% of the 16S rRNA gene amplicons at all time points in both SBRs were comprised of the 8 phyla: *Proteobacteria*, *Bacteroidetes*, *Chloroflexi*, *Nitrospirae*, *Planctomycetes*, *Verrucomicrobia*, *Acidobacteria*, and *Cyanobacteria* (Figure S9). Between 53% to 70% percent of 16S rRNA amplicons were represented by 20 genera across all samples (Figure 2). Even at the broad genus level of resolution, there were apparent differences in community profiles between the FA-treated and control SBRs over time (Figure 2), indicating that RAS treatment altered the structure of the AS microbiome.

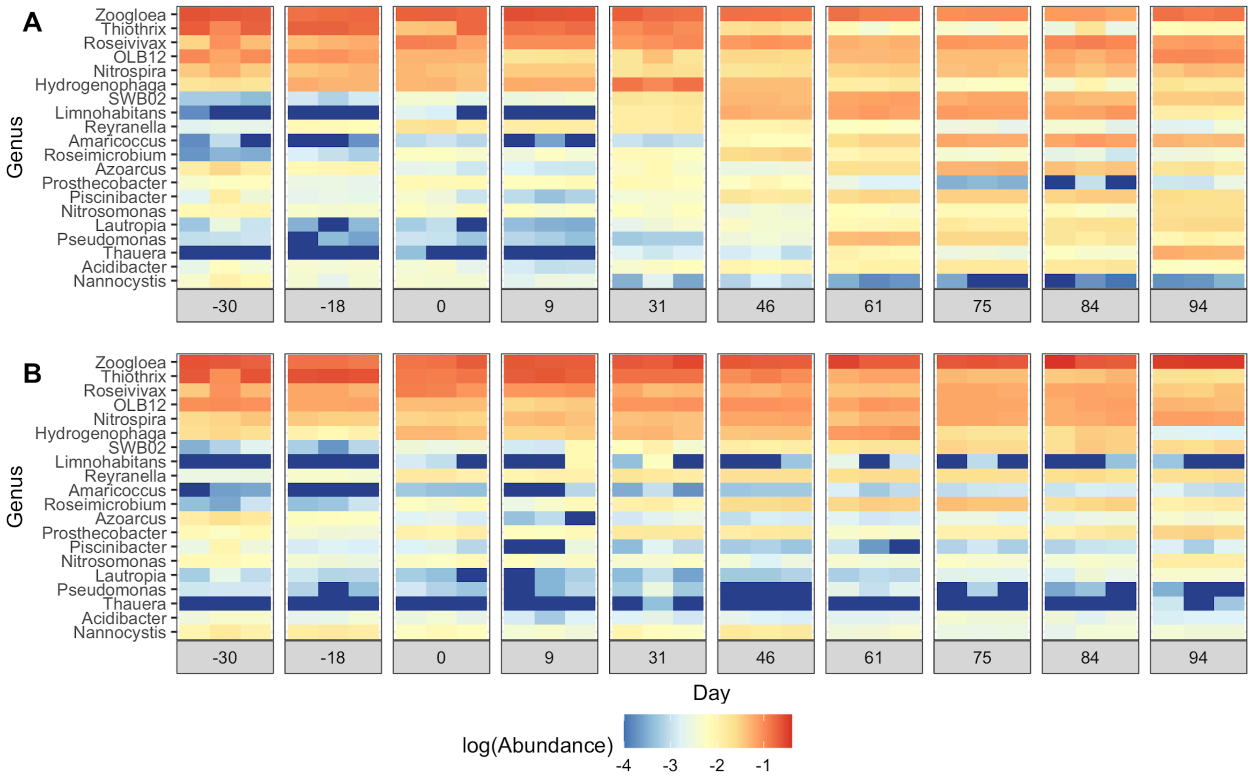

Figure 2: Heatmap of log-scaled relative abundance of top 20 most abundant genera in (A) FA-treated SBR and (B) control SBR over the two operational phases. Sequencing results are shown for triplicate DNA extractions on each sampling date. The genera are ordered from highest to lowest cumulative abundance across samples.

303 At the ASV level, FA-treatment of RAS led to significant differences in community structure
304 between the two SBRs over time (R^2 = 0.54, p < 0.001, adonis). PCA of cumulative sum-scaled
305 ASV read counts revealed that community profiles in the two SBRs were similar until day 9, after
306 which the FA-treated SBR community diverged from the control (Figure S10). Differential
307 abundance analysis showed that there were no statistically different ASVs between the two SBRs
308 on day 0 (p > 0.01, DESeq2), indicating that they were well replicated in the Non-FA Phase. By
309 day 46 of the FA-Phase, around the time that nitrite peaked in the FA-treated SBR (Figure 1), the
310 abundance of 105 ASVs spanning 55 genera were statistically different between the two SBRs (p
311 < 0.01, DESeq2; Figure S11). The number of ASVs with significant differential abundance
312 between the SBRs continued to increase to a maximum of 166 on day 75 of the FA Phase (Figure
313 S11).
314
315 *Nitrospira* and *Nitrosomonas* were the only putative NOB and AOB populations detected in the
316 SBRs, respectively (Figure 2). Eight *Nitrosomonas* ASVs were detected in both SBRs over the
317 two experimental phases (Figure S12). Until day 84, the total *Nitrosomonas* abundance was less
318 than 1% in both SBRs, but increased to over 1.5% in both by day 94 (Figure S12). One
319 *Nitrosomonas* ASV (ASV_36) was differentially abundant between the two SBRs on days 75 and
320 94 (p < 0.01, DESeq2). Three *Nitrospira* ASVs were detected within the two SBRs (Figure 3). In
321 particular, ASV_8 was the dominant *Nitrospira* ASV in both SBRs during the Start-up Phase
322 (before day 0), accounting for 3.3%±0.8% of 16S rRNA genes on average (Figure 3). By day 46,
323 ASV_8 decreased to 1.6%±0.1% in the FA-treated SBR, while it increased to 6.4%±0.3% within
324 the control. This decrease in ASV_8 abundance coincided with the peak in nitrite concentration
325 in the FA-treated SBR (Figure 1a). The abundance of ASV_8 did not significantly change after
326 day 46 for the remainder of the experiment in the FA-treated SBR (p > 0.01, DESeq2). In contrast,
327 two other *Nitrospira* ASVs (ASV_32 and ASV_47) were sporadically detected in both SBRs at
328 abundances below 0.4% until day 46, and then increased to a maximum of 1.8%±0.4% and

329 1.2%±0.3% in the FA-treated reactor by day 84, respectively, but stayed below 0.3% in the control
330 (Figure 3). The abundance of ASV_32 and ASV_47 were significantly higher in the FA reactor
331 relative to the control SBR by the end of the experiment, while ASV_8 was significantly lower
332 (both days 84 and 94; $p < 0.01$, DESeq2).
333

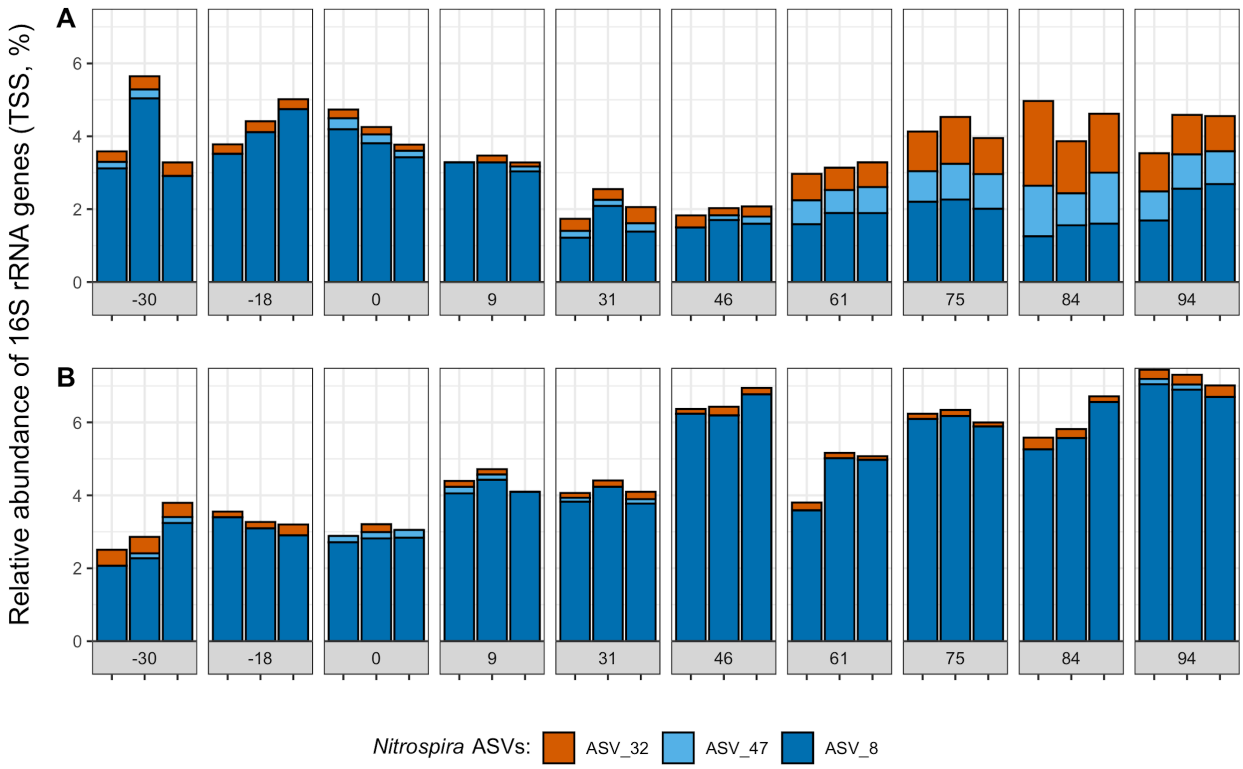

334
335 **Figure 3:** Relative abundance (total sum scaled, TSS) of three dominant *Nitrospira* ASVs over
336 time in the (A) FA-treated SBR and (B) control SBR. Only *Nitrospira* ASVs detected in more than
337 one sample are shown. Results are shown for triplicate DNA extractions on each day.
338
339
340 *3.3 Substrate analog probing of active nitrifying populations*
341
342 To decipher the impact of FA-treatment on the activity and *in situ* physiology of nitrifying
343 populations within mainstream AS, we conducted BONCAT-FACS on samples collected from
344 nitrifying microcosms seeded with mixed liquor preceding RAS treatment (R), as well as RAS
345 from the beginning (15 min after start; S1) and end (24 h after start; S2) of the side-stream
346 treatment process of each SBR (Figure 4). Preliminary validation microcosms confirmed the

347 sensitivity of BONCAT in labeling only active cells that had incorporated HPG (Figure S6).
348 Comparison of FACS data (Figures S4 and S5) between the two SBRs revealed that
349 translationally active (i.e. BONCAT+) cell fractions were significantly ($p < 0.10$) lower in nitrifying
350 microcosms seeded from the FA-treated SBR (R; 24.1% ± 2.6%, S1; 18.0% ± 3.5%, S2; 20.6% ±
351 6.3%) relative to corresponding microcosms seeded from the control SBR (R; 30.1% ± 3.8%, p =
352 0.094, S1; 28.30% ± 4.0%, p = 0.029, S2; 46.1% ± 8.2%, p = 0.015). Within the FA-treated SBR,
353 the fraction of BONCAT+ cells in the nitrifying microcosm seeded with mixed liquor (R) was
354 significantly higher than that seeded with RAS exposed to 15 min of FA-treatment (S1; p = 0.078;
355 Figure 4). However, no further reduction in the fraction of BONCAT+ cells was observed between
356 microcosms seeded with RAS from the beginning (S1) and end (S2) of the FA-treatment process
357 ($p > 0.10$). In contrast, the BONCAT+ cell fraction in the microcosm seeded with post-treated
358 RAS (S2) of the control SBR was significantly higher compared to those in its mixed liquor (R; p
359 = 0.059) and at the beginning of its RAS treatment process (S1; p=0.045; Figure 4).
360
361
362

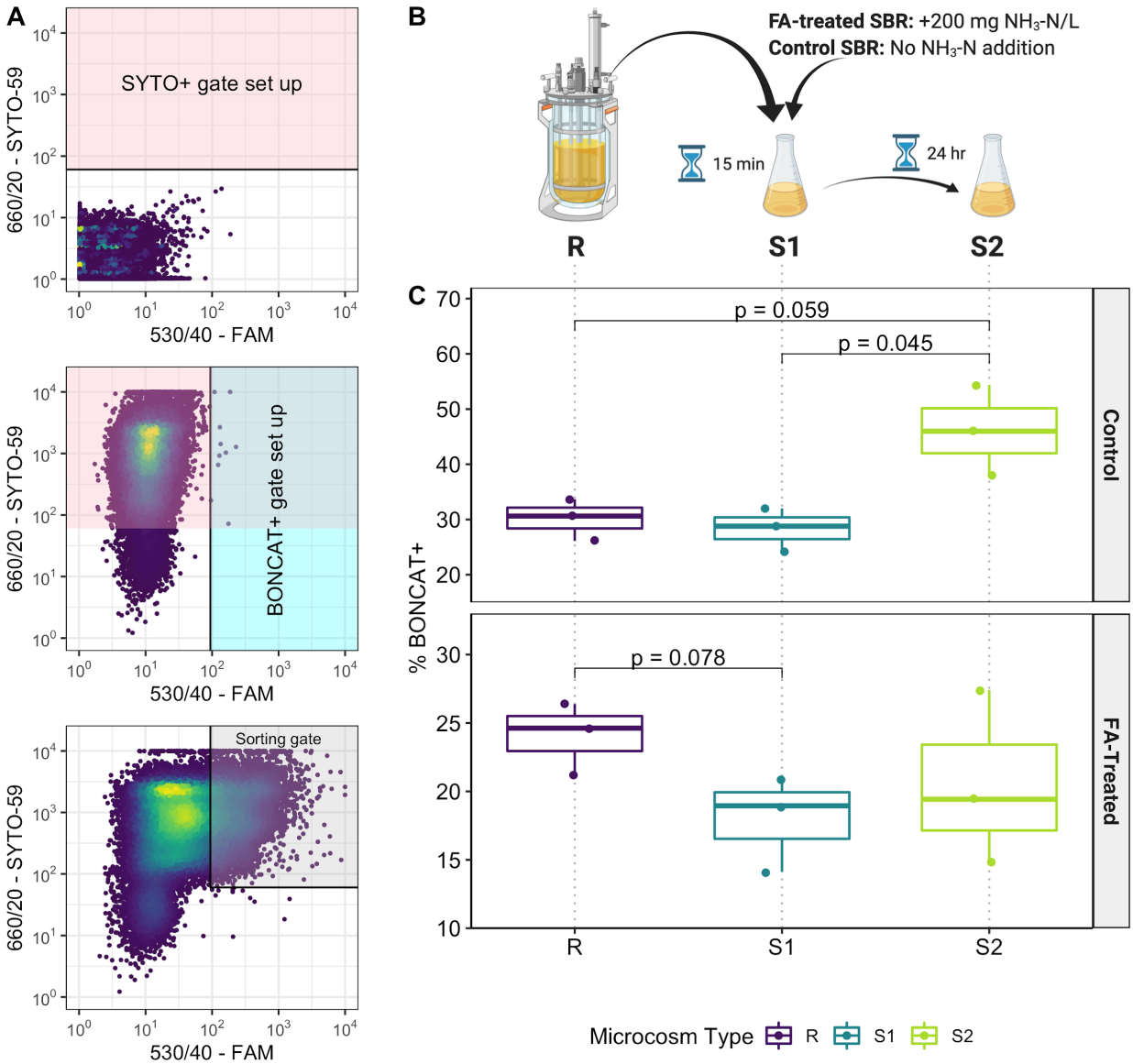

363

364 **Figure 4:** Application of BONCAT-FACS to aerobic nitrifying microcosm samples. (A) Sorting gates were
365 established based on the detection of SYTO+ cells from background particles using unstained HPG-
366 negative cells (top panel), and BONCAT+ cells from non-HPG labelled cells based on their FAM picolyl
367 azide dye fluorescence using SYTO59 stained HPG-negative cells (middle panel), allowing less than 0.5%
368 false positives in each gate. BONCAT+ cell fractions in each HPG-incubated sample were calculated as
369 the fraction of SYTO+ cells residing in the sorting gate (bottom panel). (B) Overview of the FA and control
370 RAS treatment processes showing the origin of samples used to seed the nitrifying microcosms. (C)
371 Comparison of BONCAT+ cell fractions detected in samples prepared from the nitrifying microcosms
372 seeded with mixed-liquor preceding RAS treatment (R), RAS after 15 min of side-stream treatment (S1),
373 and RAS after 24 h of side-stream treatment (S2) from the FA-treated SBR (bottom) and control SBR (top).
374 Black brackets between microcosm types are shown for differences in mean BONCAT+ cell fractions with
375 *p* values < 0.10 , as determined using independent t-tests, with calculated *p* values shown above the
376 brackets.

377 The microbial community composition observed in the BONCAT+ cell fractions can be attributed
378 to cellular translational activity, as well as any changes in bulk community composition that
379 occurred throughout the RAS treatment and sample processing steps upstream of FACS. To
380 distinguish between these impacts, we conducted 16S rRNA gene amplicon sequencing on
381 triplicate pre-homogenized and pre-sort samples from each microcosm (Figure S13), in addition
382 to control samples from HPG-negative microcosms and bulk mixed liquors prepared with different
383 DNA extraction and PCR amplification procedures (Figure S14). The low-biomass DNA extraction
384 method (prepGEM kit) and the two-step 16S rRNA gene PCR amplification, both used to prepare
385 the BONCAT microcosm libraries, showed similar impacts on community composition for both
386 SBR mixed liquors compared to respective samples prepared for time-series analysis (i.e.
387 FastDNA Soil kit with one-step PCR; Figure S15). For this reason, community composition
388 measured in the BONCAT microcosm samples were not compared to time-series samples. Within
389 the microcosm samples, pre-homogenized samples from microcosms incubated without HPG
390 were similar to those with HPG, indicating that the addition of 1 mM HPG did not significantly alter
391 community structure during the 3 h incubation (Figures S16 and S17). Pre-homogenized samples
392 from the control SBR system microcosms (R, S1 and S2) were generally clustered with the bulk
393 mixed liquor sampled directly from the SBR (Figure S17). In contrast, pre-homogenized samples
394 from the FA-treated SBR system microcosms diverged from the bulk SBR community, particularly
395 in the RAS treatment (S1 and S2) microcosms (Figure S16), suggesting that bulk community
396 composition was altered by FA-treatment. As expected, the community composition of the
397 samples after homogenization and click-chemistry labeling (i.e. pre-sort) were not identical to the
398 pre-homogenized samples, which could be attributed to cell lysis or the removal of extracellular
399 DNA present in the unfiltered samples (Couradeau et al., 2019) (Figures S16 and S17). Due to
400 these impacts, the BONCAT+ cell fractions were only compared to their corresponding bulk pre-
401 sort microcosm samples.
402

403 Comparing the abundance of taxa in a BONCAT+ cell fraction to that in its corresponding pre-sort
404 bulk community can identify changes in translational activity at the population level (Couradeau
405 et al., 2019; Reichart et al., 2020). For both the FA-treated and control SBRs, the largest distance
406 between pre-sort bulk community compositions and BONCAT+ cell fractions was observed in
407 microcosms seeded with S2 biomass from the end of RAS treatment (Figures S16 and S17).
408 Differential abundance analysis identified only 9 and 1 differentially abundant ASVs ($p < 0.01$,
409 DESeq2) in the BONCAT+ fractions of the FA-treated and control SBR mixed-liquor seeded (R)
410 microcosms, respectively, and no differentially abundant ASVs in the BONCAT+ fractions of both
411 SBR microcosms seeded with S1 biomass from the start of RAS treatment (Figure S18).
412 Conversely, for microcosms seeded with S2 biomass after 24 h of RAS treatment, 54 and 26
413 ASVs were differentially abundant in the BONCAT+ fractions of the FA-treated SBR and control
414 SBR samples, respectively (Figure S18). Within the S2 microcosm BONCAT+ fraction from the
415 FA-treated SBR, the 54 differentially abundant ASVs spanned 27 known genera, where 35% of
416 the ASVs were significantly enriched, and 65% were significantly reduced, relative to the pre-sort
417 bulk community (Figure 5). In contrast, the 26 differentially abundant ASVs identified in the S2
418 microcosm BONCAT+ fraction from the control SBR, which spanned 13 known genera, were all
419 (100%) significantly enriched relative to the pre-sort bulk community (Figure 5). These results
420 suggest that side-stream RAS treatment caused distinct shifts in the translationally active fraction
421 of the communities in both SBRs, with FA-treatment negatively impacting the activity of a greater
422 number of taxa compared to a similar anaerobic incubation without FA addition.

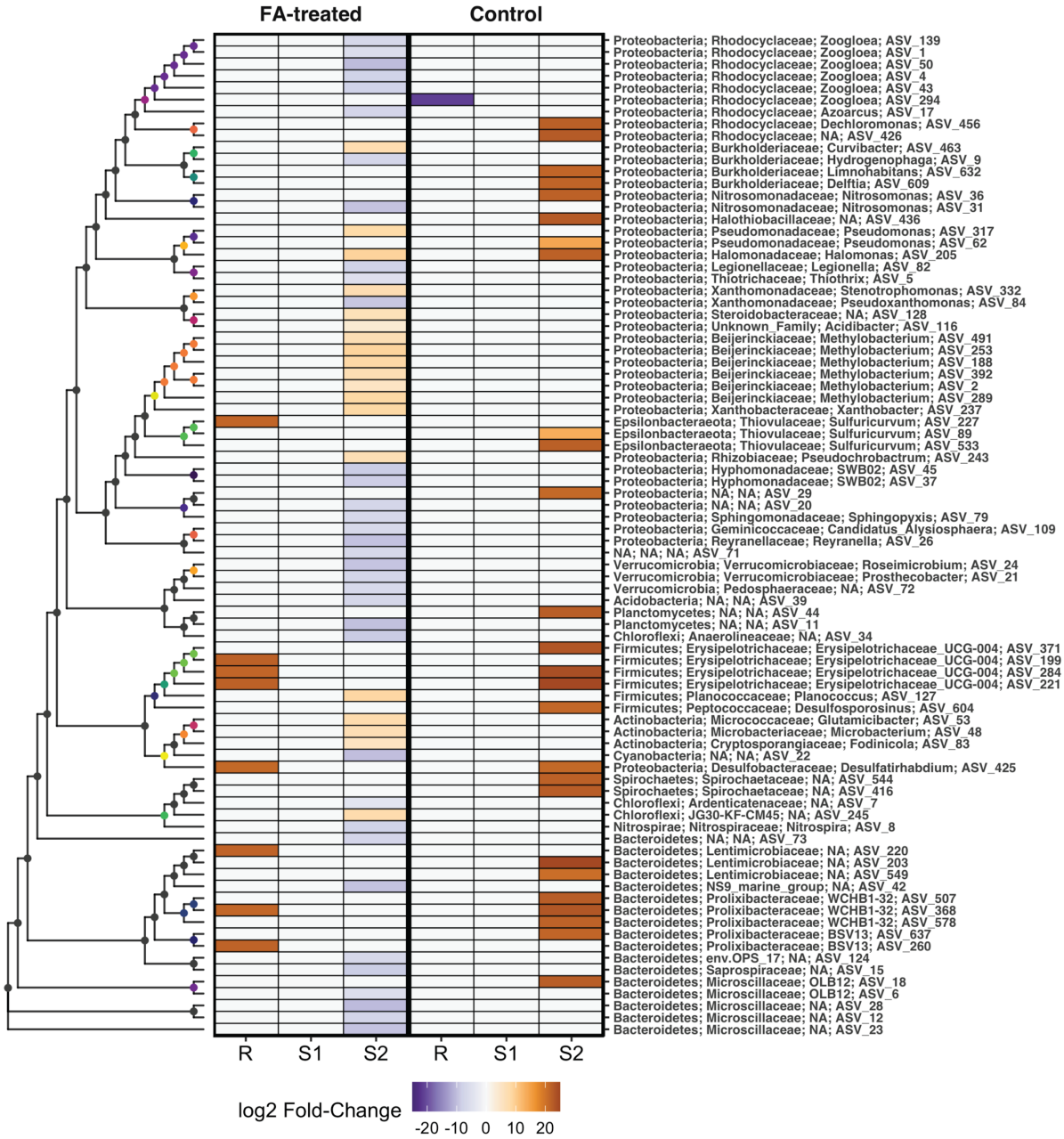

Figure 5: Log_2 fold-change in abundance of all differentially abundant ASVs detected in comparisons between BONCAT-FACS (i.e. BONCAT+) and corresponding pre-sort fractions prepared from nitrifying microcosms seeded with mixed-liquor preceding RAS-treatment (R), RAS after 15 min of side-stream treatment (S1), and RAS after 24 h of side-stream treatment (S2) from the FA-treated SBR (left panel) and control SBR (right panel). For each microcosm, log_2 fold-changes are shown only for differentially abundant ASVs, as determined by comparing ASV abundance in triplicate DNA extracts of each fraction using DESeq2 with an adjusted significance level of $p < 0.01$. Log_2 fold-changes that were not significant are set to '0' for visualization purposes. ASVs are ordered based on their phylogenetic distances estimated through multiple sequence alignment using the DECIPHER package (v.2.14.0) (Wright, 2016), and the phylogenetic tree was constructed using a maximum likelihood approach in the phangorn package (v.2.5.5) (Schliep, 2011) in the R environment. Tree tip labels (right side of the heatmap) denote the phylum, family and genus level classifications of each ASV, where NA denotes an unknown taxonomic identity at that level. Tree

436 nodes (left side of heatmap) are coloured according to genus level classification of ASVs, where nodes of
437 unknown classification (NA) are coloured grey.
438

439 As the BONCAT microcosms were amended with NH_4-N as the sole electron donor, it was
440 possible to assess the impact of RAS treatment on the translational activity of nitrifying
441 populations. The three dominant *Nitrospira* ASVs and the top two dominant *Nitrosomonas* ASVs
442 detected in both SBR BONCAT microcosm sample sets corresponded to the same dominant
443 ASVs detected in both SBR mixed liquors on day 94 of the time-series sampling, when the
444 microcosms were established (Figure 6, Figure S19). The two dominant *Nitrosomonas* ASVs
445 (ASV_31 and ASV_36) were both differentially abundant in the BONCAT+ fractions of S2
446 microcosms ($p < 0.01$, DESeq2; Figure S19), while the observed differences varied by SBR.
447 *Nitrosomonas* ASV_31 was significantly reduced in the BONCAT+ fraction of the S2-seeded
448 microcosm from the FA-treated SBR, while *Nitrosomonas* ASV_36 was significantly enriched in
449 the BONCAT+ fraction of the S2-seeded microcosm of the control SBR (Figure S19). Similar to
450 *Nitrosomonas*, the only significant differential abundance in BONCAT+ fractions for *Nitrospira*
451 ASVs occurred in a S2-seeded microcosm (Figure 6). *Nitrospira* ASV_8 was the only differentially
452 abundant NOB in BONCAT+ fractions of both SBR microcosms, and was significantly reduced in
453 the S2-seeded microcosm of the FA-treated SBR ($p < 0.01$, DESeq2). These results indicate that
454 significant reductions in translational activity of nitrifying populations were only observed in RAS
455 treated with FA.
456

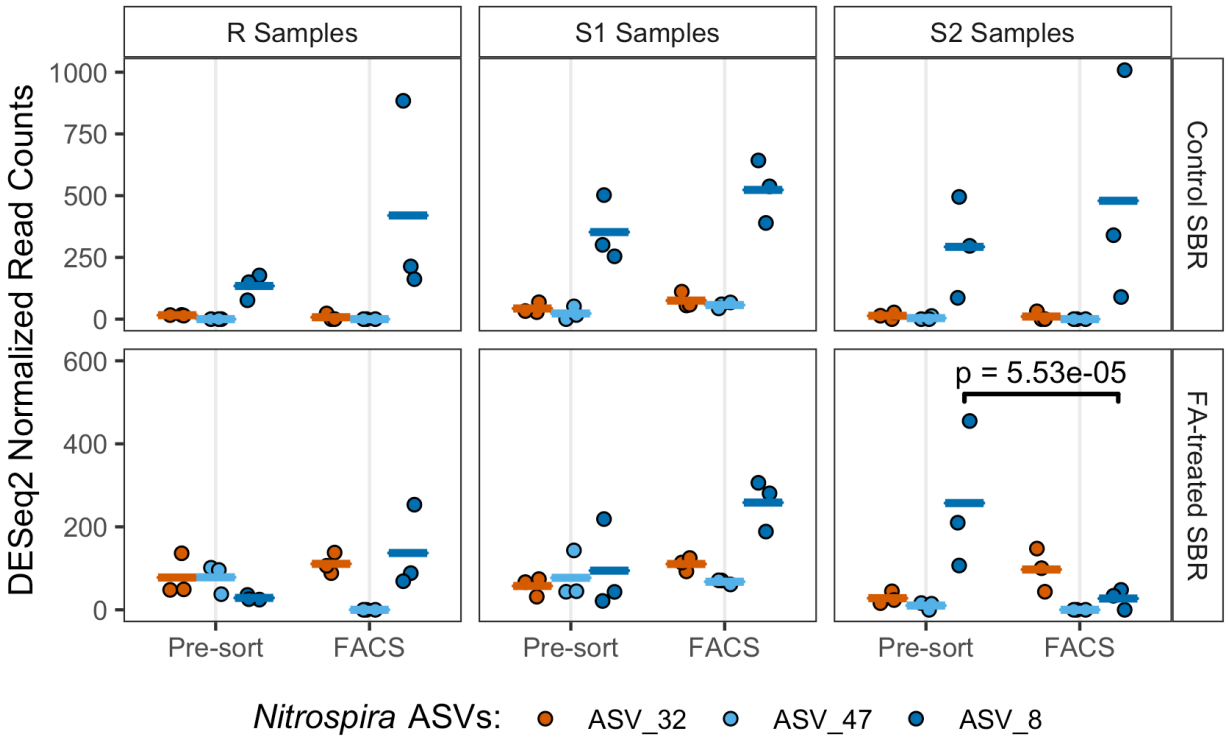

Figure 6: Normalized read counts of three dominant *Nitrospira* ASVs in triplicate BONCAT+ (i.e. FACS) and corresponding pre-sort (i.e. Pre-sort) libraries generated from samples prepared from nitrifying microcosms seeded with mixed-liquor preceding RAS treatment (R), RAS after 15 min of side-stream treatment (S1), and RAS after 24 h of side-stream treatment (S2) from the FA-treated SBR (bottom) and control SBR (top). Points indicate triplicate normalized read counts per ASV, and the horizontal bars of the same colors represent the sample mean per ASV. The reads were normalized with DESeq2 based on total read-counts per sample. A black bracket between an ASV within two samples represents a significant difference in the mean read abundance, determined with DESeq2 at an adjusted significance level of $p < 0.01$.

Discussion

The results of this study demonstrated how underlying shifts in the structure and *in situ* physiology of *Nitrospira* populations conferred the nitrite-oxidizing community with resilience to FA-based RAS treatment, and thus limited the long-term efficacy of this strategy to promote mainstream PN. We observed that a 24 h treatment of 19% of the RAS stream with 200 mg N/L as FA initially inhibited NOB activity, achieving a maximum observed NAR of 42%. However, we observed NOB acclimation to FA-treatment after approximately 40 days, in contrast to the study by Wang et al. (2017) that observed stable NARs over ~90% for over 100 days using a similar continuous FA

478 RAS treatment regime (210 mg N/L of FA for 24 hr, 22% RAS treated). NOB acclimation to FA
479 has been previously reported (Duan et al., 2019a; Li et al., 2020; Turk and Mavinic, 1989), and
480 was shown to depend on aeration duration in the mainstream AS following FA exposure (Turk
481 and Mavinic, 1989). However, very few studies have investigated the role of functional
482 degeneracy of NOB populations in supporting community-level acclimation to FA-treatment in
483 mainstream AS (Duan et al., 2019a, 2019b; Li et al., 2020). It was suggested that *Nitrospira* were
484 sensitive to FA inhibition, while *Nitrobacter* were tolerant to FA but sensitive to FNA inhibition,
485 based on a mainstream AS scenario of alternating FA and FNA RAS treatment (Duan et al.,
486 2019a). Li et al. (2020) employed continuous RAS treatment with FA in mainstream AS and found
487 that *Candidatus* Nitrogota replaced *Nitrospira* as the dominant NOB genus. In contrast to these
488 genus-level community shifts previously reported during NOB community acclimation to FA, we
489 observed that NOB acclimation could occur via shifts in different *Nitrospira* sequence variants
490 with varying sensitivities to FA. This indicates that a high-resolution analysis of 16S rRNA gene
491 amplicons was effective at capturing acclimation of key *Nitrospira* members to FA, and revealed
492 the importance of niche differentiation at the variant level for maintaining NOB out-selection in
493 mainstream PN using FA-treatment.
494
495 *Nitrospira* species are well-known to be metabolically versatile, with a wide range of functional
496 potentials including nitrite oxidation, hydrogen oxidation, urea conversion, formate oxidation,
497 nitrate reduction, and complete ammonium oxidation (Koch et al., 2014, 2015; Daims et al., 2015;
498 Bayer et al., 2020). This metabolic diversity likely creates opportunities for functionally degenerate
499 *Nitrospira* populations to co-exist within a bioreactor by differentiating in niche space through
500 auxiliary metabolic specializations, while also sharing a common niche space of nitrite oxidation.
501 Here, we employed BONCAT-FACS for the first time in a wastewater treatment system, to the
502 best of our knowledge, which highlighted differing *in situ* physiologies of three *Nitrospira* variants
503 and resolved their responses to FA-treatment on the level of cellular translational activity.

504 BONCAT-FACS revealed that transitional activity in *Nitrospira* ASV_8 was significantly reduced
505 following exposure to FA for 24 h, aligning with the results of the time-series reactor sampling in
506 which *Nitrospira* ASV_8 was washed out of the FA-treated SBR but remained dominant in the
507 control. In contrast, ASV_32 and ASV_47 increased in abundance in the FA-treated SBR
508 coinciding with the decrease in NAR after day 40, where BONCAT-FACS revealed the
509 translational activity of those variants remained unchanged following FA-treatment. It can
510 therefore be hypothesized that the out-selection of ASV_8 occurred due to its decreased
511 translational activity in response to FA-treatment, whereas potentially distinct auxiliary metabolic
512 potentials of ASV_32 and ASV_47 conferred their physiological resistance to FA, thereby
513 providing these variants with a competitive growth advantage. More broadly, the FA-treatment
514 strategy employed in this study acted as a selective pressure that impacted the stability of the
515 NOB community composition. However, functional degeneracy within the *Nitrospira* sequence
516 variants likely provided the nitrite-oxidizing community with resilience by shifting activity to
517 physiologically resistant community members. These results therefore highlight the need to
518 combine NOB out-selection approaches to effectively reduce the aggregate activity of functionally
519 degenerate and resistant NOB populations for stable mainstream PN performance. These
520 findings also underscore the need for broader applications of *in situ* physiology approaches for
521 elucidating the impacts of NOB out-selection strategies on functionally active NOB members in
522 PN systems.
523
524 Accurately measuring the active biomass fraction in biotreatment systems is critical, as many key
525 biokinetic models and process mass balances are based on active biomass concentrations
526 (Henze et al., 2000). However, conventional indirect approaches for quantifying active biomass
527 based on net substrate utilization and growth yields are unable to resolve the compositional and
528 functional dynamics of active microbial populations. As enzymes are the key catalysts that drive
529 the majority of substrate transformations in biological wastewater treatment processes, we posit

530 that measures of active biomass should be based on the translationally active microbial cell
531 fraction. The translationally active cell fractions in both SBR microcosms seeded with mixed liquor
532 measured by BONCAT-FACS (R; 24.1% ± 2.6% in FA-treated, 30.1% ± 3.8% in control) were
533 less than the active biomass fraction predicted through steady-state modeling (Metcalf & Eddy,
534 Inc. et al., 2013) (67-77% VSS-basis; Supplementary Information), which is likely because the
535 microcosms were only supplemented with ammonium as an electron donor. Nonetheless, we
536 observed many translationally active heterotrophs in the BONCAT microcosms, which could have
537 remained active through metabolism of internal carbon reserves, endogenous respiration, or
538 constitutive protein expression. The consistent increase in translational activity across all
539 differentially abundant ASVs detected in the BONCAT+ fraction of the microcosm seeded with
540 control SBR RAS following the 24 h incubation could thus have been attributed to fermentative
541 metabolism on cell decay products. In contrast, the mixed translational responses of differentially
542 abundant ASVs in the BONCAT+ fraction of the RAS microcosm following incubation with FA
543 suggests that more complex dynamics between cellular inhibition, decay, and fermentative
544 metabolism were induced by FA-treatment. This analysis highlights the value of BONCAT as an
545 *in situ* physiology approach to directly measure concentrations of translationally active population
546 members in AS under various reactor configurations, which could be extended to resolve
547 associations of activity in AS taxa with different substrate preferences (Reichart et al., 2020) or to
548 validate biokinetic parameters. As higher-resolution process modeling of active populations has
549 been called for to optimize A-B processes that rely on community modulation and/or interactions
550 between functional groups (e.g. PN, PN-A) (Agrawal et al., 2018), *in situ* physiology approaches
551 like BONCAT will likely play a key role in developing the next-generation of wastewater treatment
552 technologies.
553
554
555

556 **Conclusions**

557 Achieving consistent out-selection of NOB in mainstream AS remains as a key challenge towards
558 the maintenance of stable PN for energy-efficient BNR processes. This study investigated the
559 underlying mechanisms providing nitrite-oxidizing communities in AS bioreactors with resilience
560 to out-selection during the treatment of a fraction of RAS with a sidestream flow containing high
561 concentrations of FA, similar to anaerobic digester centrate. Sidestream FA-treatment of RAS
562 was shown to promote nitrite accumulation in AS under mainstream conditions; however, the
563 effects were transient. The acclimation of the nitrite oxidizing community to repeated FA treatment
564 was attributed to resistant *Nitrospira* populations that increased in abundance over time. The *in-*
565 *situ* physiological responses of different *Nitrospira* populations were measured throughout FA
566 exposure using BONCAT-FACS activity-based cell sorting, and corroborated their observed time-
567 series abundance dynamics in the AS bioreactor. Therefore, closely-related *Nitrospira*
568 populations co-existing within the same AS bioreactor had differing physiological responses to
569 the applied out-selection pressure, conferring resilience to the nitrite oxidation process and
570 causing deterioration of PN performance. Due to this observed functional degeneracy in *Nitrospira*
571 populations, we recommended the concerted application of multiple NOB out-selection strategies
572 that impact physiologically diverse NOB to achieve stable PN in mainstream AS.

573

574

575
576
577
578
579
580
581
582
583
584
585

Acknowledgements

This work was supported by the Natural Sciences and Engineering Research Council (NSERC) of Canada (Discovery Grant). MM was supported by an NSERC CGS-M fellowship.

Author Information

MM and YL contributed equally to this work.

Supplementary Information

The Supplementary Information file contains supplemental notes pertaining to detailed materials and methods, bioinformatics scripts, Tables S1-S12, and Figures S1-20.

References

Agrawal, S., Seuntjens, D., Cocker, P.D., Lackner, S., Vlaeminck, S.E., 2018. Success of mainstream partial nitritation/anammox demands integration of engineering, microbiome and modeling insights. Curr. Opin. Biotechnol. 50, 214–221. https://doi.org/10.1016/j.copbio.2018.01.013

Bayer, B., Saito, M.A., McIlvin, M.R., Lücker, S., Moran, D.M., Lankiewicz, T.S., Dupont, C.L., Santoro, A.E., 2020. Metabolic versatility of the nitrite-oxidizing bacterium Nitrospira marina and its proteomic response to oxygen-limited conditions. ISME J. 1–15. https://doi.org/10.1038/s41396-020-00828-3

Callahan, B.J., McMurdie, P.J., Rosen, M.J., Han, A.W., Johnson, A.J.A., Holmes, S.P., 2016. DADA2: High-resolution sample inference from Illumina amplicon data. Nat. Methods 13, 581–583. https://doi.org/10.1038/nmeth.3869

Cao, Y., van Loosdrecht, M.C.M., Daigger, G.T., 2017. Mainstream partial nitritation–anammox in municipal wastewater treatment: status, bottlenecks, and further studies. Appl. Microbiol. Biotechnol. 101, 1365–1383. https://doi.org/10.1007/s00253-016-8058-7

Cogert, K.I., Ziels, R.M., Winkler, M.K.H., 2019. Reducing Cost and Environmental Impact of Wastewater Treatment with Denitrifying Methanotrophs, Anammox, and Mainstream Anaerobic Treatment. Environ. Sci. Technol. 53, 12935–12944. https://doi.org/10.1021/acs.est.9b04764

Couradeau, E., Sasse, J., Goudeau, D., Nath, N., Hazen, T.C., Bowen, B.P., Chakraborty, R., Malmstrom, R.R., Northen, T.R., 2019. Probing the active fraction of soil microbiomes using BONCAT-FACS. Nat. Commun. 10, 2770. https://doi.org/10.1038/s41467-019-10542-0

Daims, H., Lebedeva, E.V., Pjevac, P., Han, P., Herbold, C., Albertsen, M., Jehmlich, N., Palatinszky, M., Vierheilig, J., Bulaev, A., Kirkegaard, R.H., von Bergen, M., Rattei, T., Bendinger, B., Nielsen, P.H., Wagner, M., 2015. Complete nitrification by Nitrospira bacteria. Nature 528, 504–509. https://doi.org/10.1038/nature16461

Daims, H., Lücker, S., Wagner, M., 2016. A New Perspective on Microbes Formerly Known as Nitrite-Oxidizing Bacteria. Trends Microbiol. 24, 699–712. https://doi.org/10.1016/j.tim.2016.05.004

Duan, H., Wang, Q., Erler, D.V., Ye, L., Yuan, Z., 2018. Effects of free nitrous acid treatment conditions on the nitrite pathway performance in mainstream wastewater treatment. Sci. Total Environ. 644, 360–370. https://doi.org/10.1016/j.scitotenv.2018.06.346

Duan, H., Ye, L., Lu, X., Yuan, Z., 2019a. Overcoming Nitrite Oxidizing Bacteria Adaptation through Alternating Sludge Treatment with Free Nitrous Acid and Free Ammonia. Environ. Sci. Technol. 53, 1937–1946. https://doi.org/10.1021/acs.est.8b06148

Duan, H., Ye, L., Wang, Q., Zheng, M., Lu, X., Wang, Z., Yuan, Z., 2019b. Nitrite oxidizing bacteria (NOB) contained in influent deteriorate mainstream NOB suppression by sidestream inactivation. Water Res. 162, 331–338. https://doi.org/10.1016/j.watres.2019.07.002

Eren, A.M., Morrison, H.G., Lescault, P.J., Reveillaud, J., Vineis, J.H., Sogin, M.L., 2015. Minimum entropy decomposition: Unsupervised oligotyping for sensitive partitioning of high-throughput marker gene sequences. ISME J. 9, 968–979. https://doi.org/10.1038/ismej.2014.195

Ge, S., Peng, Y., Qiu, S., Zhu, A., Ren, N., 2014. Complete nitrogen removal from municipal wastewater via partial nitrification by appropriately alternating anoxic/aerobic conditions in a continuous plug-flow step feed process. Water Res. 55, 95–105. https://doi.org/10.1016/j.watres.2014.01.058

Hahne, F., LeMeur, N., Brinkman, R.R., Ellis, B., Haaland, P., Sarkar, D., Spidlen, J., Strain, E.,

Gentleman, R., 2009. flowCore: a Bioconductor package for high throughput flow cytometry. BMC Bioinformatics 10, 106. https://doi.org/10.1186/1471-2105-10-106

Hatzenpichler, R., Connon, S.A., Goudeau, D., Malmstrom, R.R., Woyke, T., Orphan, V.J., 2016. Visualizing in situ translational activity for identifying and sorting slow-growing archaeal−bacterial consortia. Proc. Natl. Acad. Sci. 113, E4069–E4078. https://doi.org/10.1073/pnas.1603757113

Hatzenpichler, R., Krukenberg, V., Spietz, R.L., Jay, Z.J., 2020. Next-generation physiology approaches to study microbiome function at single cell level. Nat. Rev. Microbiol. https://doi.org/10.1038/s41579-020-0323-1

Hatzenpichler, R., Scheller, S., Tavormina, P.L., Babin, B.M., Tirrell, D.A., Orphan, V.J., 2014. *In situ* visualization of newly synthesized proteins in environmental microbes using amino acid tagging and click chemistry: Visualizing new proteins in microbes by click chemistry. Environ. Microbiol. 16, 2568–2590. https://doi.org/10.1111/1462-2920.12436

Henze, M., Gujer, W., Mino, T., Loosdrecht, M.C.M. van, 2000. Activated sludge models ASM1, ASM2, ASM2d and ASM3. IWA Publishing.

Koch, H., Galushko, A., Albertsen, M., Schintlmeister, A., Gruber-Dorninger, C., Lücker, S., Pelletier, E., Paslier, D.L., Spieck, E., Richter, A., Nielsen, P.H., Wagner, M., Daims, H., 2014. Growth of nitrite-oxidizing bacteria by aerobic hydrogen oxidation. Science 345, 1052–1054. https://doi.org/10.1126/science.1256985

Koch, H., Lücker, S., Albertsen, M., Kitzinger, K., Herbold, C., Spieck, E., Nielsen, P.H., Wagner, M., Daims, H., 2015. Expanded metabolic versatility of ubiquitous nitrite-oxidizing bacteria from the genus Nitrospira. Proc. Natl. Acad. Sci. 112, 11371–11376. https://doi.org/10.1073/pnas.1506533112

Kornaros, M., Dokianakis, S.N., Lyberatos, G., 2010. Partial Nitrification/Denitrification Can Be Attributed to the Slow Response of Nitrite Oxidizing Bacteria to Periodic Anoxic Disturbances. Environ. Sci. Technol. 44, 7245–7253. https://doi.org/10.1021/es100564j

Li, S., Duan, H., Zhang, Y., Huang, X., Yuan, Z., Liu, Y., Zheng, M., 2020. Adaptation of nitrifying community in activated sludge to free ammonia inhibition and inactivation. Sci. Total Environ. 728, 138713. https://doi.org/10.1016/j.scitotenv.2020.138713

Li, X., Klaus, S., Bott, C., He, Z., 2018. Status, Challenges, and Perspectives of Mainstream Nitritation-Anammox for Wastewater Treatment. Water Environ. Res. 90, 634–649. https://doi.org/10.2175/106143017X15131012153112

Liu, G., Wang, J., 2013. Long-Term Low DO Enriches and Shifts Nitrifier Community in Activated Sludge. Environ. Sci. Technol. 47, 5109–5117. https://doi.org/10.1021/es304647y

Love, M.I., Huber, W., Anders, S., 2014. Moderated estimation of fold change and dispersion for RNA-seq data with DESeq2. Genome Biol. 15, 550. https://doi.org/10.1186/s13059-014-0550-8

Lücker, S., Schwarz, J., Gruber-Dorninger, C., Spieck, E., Wagner, M., Daims, H., 2015. Nitrotoga-like bacteria are previously unrecognized key nitrite oxidizers in full-scale wastewater treatment plants. ISME J. 9, 708–720. https://doi.org/10.1038/ismej.2014.158

Metcalf & Eddy, Inc., Tchobanoglous, G., Burton, F., Stensel, H.D., 2013. Wastewater Engineering: Treatment and Resource Recovery, 5th ed. McGraw-Hill.

Nierychlo, M., Andersen, K.S., Xu, Y., Green, N., Jiang, C., Albertsen, M., Dueholm, M.S., Nielsen, P.H., 2020. MiDAS 3: An ecosystem-specific reference database, taxonomy and knowledge platform for activated sludge and anaerobic digesters reveals species-level microbiome composition of activated sludge. Water Res. 115955. https://doi.org/10.1016/j.watres.2020.115955

Oksanen, J., Kindt, R., Legendre, P., O'Hara, B., Stevens, M.H.H., Oksanen, M.J., Suggests, M., 2007. The vegan package. Community Ecol. Package 10, 719.

Parada, A.E., Needham, D.M., Fuhrman, J.A., 2016. Every base matters: assessing small subunit rRNA primers for marine microbiomes with mock communities, time series and global field samples. Environ. Microbiol. 18, 1403–1414. https://doi.org/10.1111/1462-2920.13023

Paulson, J.N., Stine, O.C., Bravo, H.C., Pop, M., 2013. Differential abundance analysis for microbial marker-gene surveys. Nat. Methods 10, 1200–1202. https://doi.org/10.1038/nmeth.2658

Regmi, P., Miller, M.W., Holgate, B., Bunce, R., Park, H., Chandran, K., Wett, B., Murthy, S., Bott, C.B., 2014. Control of aeration, aerobic SRT and COD input for mainstream nitritation/denitritation. Water Res. 57, 162–171. https://doi.org/10.1016/j.watres.2014.03.035

Reichart, N.J., Jay, Z.J., Krukenberg, V., Parker, A.E., Spietz, R.L., Hatzenpichler, R., 2020. Activity-based cell sorting reveals responses of uncultured archaea and bacteria to substrate amendment. ISME J. https://doi.org/10.1038/s41396-020-00749-1

Schliep, K.P., 2011. phangorn: phylogenetic analysis in R. Bioinformatics 27, 592–593. https://doi.org/10.1093/bioinformatics/btq706

Singer, E., Wagner, M., Woyke, T., 2017. Capturing the genetic makeup of the active microbiome in situ. ISME J. 11, 1949–1963. https://doi.org/10.1038/ismej.2017.59

Spasov, E., Tsuji, J.M., Hug, L.A., Doxey, A.C., Sauder, L.A., Parker, W.J., Neufeld, J.D., 2019. High functional diversity among *Nitrospira* populations that dominate rotating biological contactor microbial communities in a municipal wastewater treatment plant (preprint). Microbiology. https://doi.org/10.1101/529826

Tang, J., Landes, R.D., 2020. Some t-tests for N-of-1 trials with serial correlation. PLOS ONE 15, e0228077. https://doi.org/10.1371/journal.pone.0228077

Turk, O., Mavinic, D.S., 1989. Stability of Nitrite Build-Up in an Activated Sludge System. J. Water Pollut. Control Fed. 61, 1440–1448.

Wang, Q., Duan, H., Wei, W., Ni, B.-J., Laloo, A., Yuan, Z., 2017. Achieving Stable Mainstream Nitrogen Removal via the Nitrite Pathway by Sludge Treatment Using Free Ammonia. Environ. Sci. Technol. 51, 9800–9807. https://doi.org/10.1021/acs.est.7b02776

Wang, Q., Garrity, G.M., Tiedje, J.M., Cole, J.R., 2007. Naïve Bayesian Classifier for Rapid Assignment of rRNA Sequences into the New Bacterial Taxonomy. Appl. Environ. Microbiol. 73, 5261–5267. https://doi.org/10.1128/AEM.00062-07

Wickham, H., Averick, M., Bryan, J., Chang, W., McGowan, L.D., François, R., Grolemund, G., Hayes, A., Henry, L., Hester, J., Kuhn, M., Pedersen, T.L., Miller, E., Bache, S.M., Müller, K., Ooms, J., Robinson, D., Seidel, D.P., Spinu, V., Takahashi, K., Vaughan, D., Wilke, C., Woo, K., Yutani, H., 2019. Welcome to the Tidyverse. J. Open Source Softw. 4, 1686. https://doi.org/10.21105/joss.01686

Wright, E., S., 2016. Using DECIPHER v2.0 to Analyze Big Biological Sequence Data in R. R J. 8, 352. https://doi.org/10.32614/RJ-2016-025

Xu, G., Zhou, Y., Yang, Q., Lee, Z.M.-P., Gu, J., Lay, W., Cao, Y., Liu, Y., 2015. The challenges of mainstream deammonification process for municipal used water treatment. Appl. Microbiol. Biotechnol. 99, 2485–2490. https://doi.org/10.1007/s00253-015-6423-6